ANALYSIS OF THERMAL AND IRRADIATION BEHAVIOUR OF FUELLED GRAPHITE BRICKS FOR A HIGH TEMPERATURE GAS COOLED REACTOR

V.S. BECKETT,

British Nuclear Design and Construction Ltd.,
Whetstone, Leicester, United Kingdom

ABSTRACT

The fuelled moderator bricks which structurally make up the core of the B.N.D.C. H.T.R. design are described and analyses are given of the various design considerations necessary to ensure acceptable performance of the bricks with respect to their thermal and irradiation behaviour. Typical analyses are presented in the form of figures and tables.

1. INTRODUCTION

The main features of the B.N.D.C. H.T.R. design have been recently described by Tyrrell and Lowthian (1) and Insch et al (2). The core consists of a stable arrangement of hexagonal graphite columns, the basic unit being a brick of approximately one metre length and of hexagonal cross-section with an across flats dimension of half a metre. Each of these columns contain 24 fuel channels into which are inserted the fuel pins. The fuel pin consists of annular compacts of coated particle fuel enclosed within inner and outer graphite fuel tubes. The outer tube is provided with three integral ribs to locate and stabilise the fuel pin centrally within the fuel channel. The coolant flow is downward through the centre of the fuel pin and also through the annular passage formed by the outer fuel tube and the fuel channel.

Each moderator brick contains a central hole which is provided with a lifting feature and which can also be used to accommodate a control rod. The bricks are stacked to form the columns and spigoted and dowelled at their ends to provide respectively central and azimuthal location with respect to those bricks vertically adjacent. The columns fit closely only at location planes above and below the fuelled column length; within the active core the intercolumn gap is sized to prevent interaction between adjacent columns due to irradiation induced distortion. The following design aspects of the graphite bricks which describe their thermal and irradiation behaviour are considered here;-

a) Temperature analysis
b) Thermal elastic stress analysis

c)Irradiation induced shrinkage - creep stress analysis

d)Bowing of brick columns

e)Brick end face distortion

2. TEMPERATURE ANALYSIS

It is important to determine temperature distributions within fuel bricks not only to enable derivation of the thermal stresses but also to be able to ascribe material properties to any particular region of the brick. This is important in assessing both corrosion rates in specific weight loss sensitive areas and also the levels of irradiation induced shrinkage and creep rates.

During their operative life the thermal conditions applied to the fuel bricks are -

- Internal heat generation due to nuclear heating
- A gas stream of axially varying temperature through the feed channels
- Cooling gas flow around the bricks and through control rod channels.

There are two stages in the calculation of brick temperature distribution. These are firstly an assessment of the boundary conditions and heat loads within and around the brick and secondly, solution of the conduction problem within the brick. Within this framework there are a number of possible methods of solution each varying in the degree of sophistication employed. With a problem of this complexity a solution by classical analytical techniques is obviously out of the question. Of the numerical methods available the finite element technique in particular lends itself to this problem because of the ease with which complicated boundary shapes and discontinuities of material properties can be handled. The basic program used in the thermal analysis was a two dimensional heat conduction code for plane bodies using triangular elements. The boundary conditions could be specified as body temperatures or heat transfer coefficients. Internal heat generation could be proscribed to any node. This programme is one of a suite of finite element programmes, the others dealing with stress analysis and these are described by Miles and White (3). To obtain solutions for any plane axially within a brick column the boundary conditions are adjusted to simulate conditions at that plane. Particular solutions obtained from this two dimensional code have been compared with those derived from a code developed by the United Kingdom Atomic Energy Authority referred to as PERCON. This again is a finite element code but as well as obtaining two dimensional solutions of temperature it can connect these planes by a flowing coolant. It has a number of special facilities which make it applicable to fuel element analysis. For instance certain heat transfer correlations can be specified for connecting the planes with the coolant and also one overall coolant flow can be specified for a number of fuel channels together with the power of each channel and the axial variation of power. The program can then ascribe mass flows to each channel and obtain solutions at specified axial planes down the length of the core. When outlet coolant conditions are obtained pressure drops are calculated and the inlet mass flow distribution re-ascribed for an overall pressure loop iteration.

The model considered for the two dimensional code is a mesh of triangular elements covering half of the cross-sectional area of the fuel brick with an insulated boundary across the corners of the hexagon. Heat inputs are ascribed to each node of the mesh to represent the graphite heat generation rates and boundary conditions applied as heat transfer coefficients and coolant gas temperatures. The mesh consists of 407 elements and 296 nodes with small triangles covering the critical areas between fuel channels and around the central hole with larger triangles around the low heat flux boundary of the brick periphery.

For the PERCON program the cross-sectional planes are represented by the same mesh as above with additional elements representing a simplified fuel pin. Each annulus in the fuel channel is represented as 12 coolant sub-channels not directly connected to each other by a heat path. Input data consists of fuel channel powers, axial power distributions, graphite heat generation as a proportion of total block power, total coolant mass flow and inlet coolant temperature. Results have been obtained for six axial planes after one pressure loop iteration.

Since the active core of the main line B.H.D.C. H.T.R. design consists of a large number of fuelled columns, it is obviously undesirable to carry out detailed analysis of the type described above on all of them. Judgment is, therefore, necessary to decide the potentially critical regions of the core, with respect to high thermal gradients. Two columns have been chosen for analysis:

i) Central core column - The reason for this choice is that it is a high powered column with an operating control rod in the central hole. This combination will obviously involve high levels of temperature in the outer ring of fuel channels and high temperature gradients towards the central hole.

ii) A fuel column on the periphery of the active core - Again this contains an operating control rod but also sustains a high power gradient across itself by virtue of its position at the edge of the core.

A considerable number of temperature solutions have been obtained for these cases during the period of core design and performance optimisation, examples of which are shown in Figures 1 and 2. Figure 1 shows temperature contours for the cross-sectional plane at the bottom of the active core for the peripheral fuel column case. The conditions in the central hole are such that the control rod is partially inserted and the control rod cooling flow is developed across the whole flow area of the channel. This is seen to produce temperature gradients radial to the centre of the brick together with across brick gradients resulting from power variation across the brick. Figure 2 shows a similar distribution for the central column case, but in this case the control rod is fully inserted thereby providing a suppression of the powers of the inner ring of fuel pins. This power tilt is applied radially from the centre of the brick resulting in azimuthal variations of gas temperature as shown in Figure 2.

Comparison between the results derived from the two calculation models described above indicates that the errors involved in the use of the two-dimensional code are a maximum in the regions between fuel channels in the presence of large channel power gradients. This is principally due to the fact that the boundary conditions for each fuel channel are calculated independently of the local channel to channel power gradient. The result is an over-estimate of temperature gradients between channels of different powers,

as the integrated effect axially of heat flow between these channels is taken into account only in the PERCON model.

3. THERMAL ELASTIC STRESS ANALYSIS

As seen in Figures 1 and 2, considerable temperature gradients can exist through cross sectional planes of a fuel brick either as a result of across brick power gradients or the presence of high cooling flows in the central hole. This section deals with the stress levels which are produced as a result of these temperature gradients. In all the calculations, the effect of axial temperature variations on the stress levels have been considerd negligible compared with the cross sectional temperature gradients which are much greater.

The basic method employed has been to use the temperatures obtained in the previously described thermal analysis as input to a finite element program which is in fact another program of the same family as the temperature program. These programs are very versatile incorporating a Choleski solve-equations routine, ref.(3). In the stress analysis runs obtained from the temperature distributions the nodal displacements and element stresses are obtained in two minutes on an English Electric KDF 9 Computer. Also programs have been combined such that it is possible to solve for the temperature distribution and continue with the thermal stress calculation.

The same element mesh distribution has been used for the stress solutions and the only external constraints applied are that nodes on the line of symmetry of the hexagon are constrained to move along this line with no orthogonal component. There are two possible two dimensional solutions which can be used to give approximate solutions to a three dimensional problem:-

i) Plane Stress: This is in fact a true two dimensional state of stress where the stresses normal to the plane are zero, and in the usual convention:

$$\sigma_{zz} = \sigma_{xz} = \sigma_{yz} = 0 \qquad \text{eq (1)}$$

This can be considered an adequate solution for the case of a thin plate with an in-plane temperature gradient and with the surfaces free of tractions.

ii) Plane Strain: This condition is achieved by assuming displacements in the normal direction to be zero and that displacements in the other directions are independent of the normal direction. In this case:

$$\sigma_{xz} = \sigma_{yz} = 0 \qquad \text{eq (2)}$$

This condition occurs in a prismatic body whose length is very large compared with its cross-sectional dimensions and whose temperatures and loads are independent of the z - direction.

In the H.T.R. core the fuel bricks are 500 mm A/F and 1000 mm length with large temperature gradients in the xy plane. To obtain a rigorous stress solution for such a body requires a three dimensional analysis since the length of the block is neither very large nor very small in relation to its width. Nevertheless the two stress systems defined above can be used and whereas it may be assumed that the plane stress solution under estimates the real stresses for most regions of the block except possibly for the end faces, it is equally true that the constraints resulting from a plane strain assumption are more severe than those occurring in reality.

Most of the stress analysis has been performed for the case of plane strain concentrating on the lower 40% of the active core where the greater temperature gradients occur. Two cases are analysed below corresponding to the temperature distributions given previously.

a) Peripheral Column:- Control rod withdrawn.
The temperature distribution for this case is given in Figure 1 and the resulting xy thermal elastic stress distribution is shown in Figure 3 based on the plane strain assumption. Maximum principal tensile stresses have been plotted in magnitude and direction for each element of the mesh for values exceeding $1N/mm^2$.
It can be seen that the direction of these stresses generally tend to follow the temperature contours as expected with maximum values of about $6N/mm^2$ around the central hole. For comparison Figure 4 is included which gives the same solution, but for the case of plane stress. It can be seen that this results in a reduction of the stress values of about 15%.

b) Centre Column:- Control rod inserted.
The temperature distribution for this case is shown in Figure 2 and the resulting stress distribution obtained from a 'plane strain' calculation is presented in Figure 5. In this case it is seen that high stresses exist in the ligaments between fuel channels as a result of the higher gas temperature differentials between adjacent channels.

It has been stated earlier that the temperature gradients through the ligaments between inner and outer rings of fuel channels are exaggerated due to the fact that boundary gas temperatures have been calculated independently of the channel to channel power gradient. It is reasonable to assume, therefore, that the peak stresses quoted for this region will be reduced for the real case.

In order to examine the sensitivity of thermal stresses in the brick to changes in the coolant flow the temperature analysis of Figure I has been repeated for an arbitrary increase of 15% in the central hole flow. The effect of this flow on the temperature distribution is confined to the immediate area of the central hole and on average the temperature difference between the central hole wall and the adjacent regions of the inner ring of fuel channels is increased by $20^{\circ}C$. The effect on the stress distribution is likewise confined to the ligament around the central hole with the loop stresses around the channel wall increase by 13%.

The graphite properties used in the above analysis are those for a moulded isotropic gilso-carbon graphite. As material properties have not varied from element to element for any particular planar solution the thermal stresses can be considered as being given by:

$$\sigma_i = C \alpha E \qquad \text{eq (3)}$$

where: σ_i = stress in i^{th} element
α = coefficient of thermal expansion
E = Young's Modulus
C = Constant for a particular temperature distribution

therefore when considering any variation in properties of a particular graphite the thermal stresses can be obtained by scaling according to equation (3).

On starting up the reactor, temperature gradients are set up within the fuel bricks as discussed earlier and these gradients give rise to thermal stresses which have been determined for a new fuel column. These early life thermal stresses quickly creep out due to stress relaxation as irradiation proceeds and compatibility will be maintained by the formation of a system of creep strains. In the event of shutdown of the reactor these initial distributions of thermal stress reappear with opposite sign as the temperature gradients disperse. The magnitude of these stresses for the shutdown condition can be determined by scaling the early life thermal stresses in the ratio of $E.\alpha$ (i.e. Youngs Modulus and thermal expansion coefficient for the two conditions). This assumes that the temperature distribution just before shutdown is the same as the early life distribution and that the initial thermal stresses have fully relaxed out before shutdown occurs.

Damaging effects of thermal stresses on the fuel brick will occur if the tensile stresses exceed the ultimate tensile strength of the material. Cracks can then occur local to these stresses assuming there is insufficient yield in the material to dissipate the stresses as plastic strains to an extent sufficient to reduce the stress levels to below the local ultimate tensile strength (U.T.S.) of the material.

If stresses reach the level of the material U.T.S. this will only occur in localised regions of the brick for two reasons. Firstly the high levels of thermal stress are themselves localised to specific regions of the brick where the maximum temperature gradients exist. Secondly, for even the highest stresses obtained in the present series of calculations to exceed the U.T.S. that U.T.S. must be considerably below the bulk guaranteed value. This could only occur in areas of local weakness and would more than likely represent a specific flaw in the material. Steady state elastic stress systems only exist at their peak values for a short time at beginning of fuel life and so such cracks would not propagate beyond their opening condition. At shutdown the cracks would close up due to the fact that the stresses that caused them to open would be reversed.

4. IRRADIATION INDUCED SHRINKAGE - CREEP STRESS ANALYSIS

It is stated earlier that the initial elastic thermal stresses will relax out fairly rapidly as irradiation proceeds. While this occurs another system of stresses will develop as a result of differential irradiation induced (or Wigner) shrinkage across fuel bricks particularly those on the periphery of the core situated in regions of high fast neutron flux gradients. A steady state situation will eventually be attained where these differential strains create sufficiently high stress levels to maintain a balancing secondary creep rate.

This section is concerned with calculating the resulting stress system.

The solutions obtained prreviously to the thermal elastic problem, are derived from the multiaxial stress equations of the form:

$$\varepsilon_z = \alpha T + \frac{1}{E}[\sigma_z - \nu(\sigma_x + \sigma_y)] \qquad \text{eq. (4)}$$

where ε_z is z coordinate strain, α is coefficient of thermal expansion, T is temperature, E is Young's Modulus, $\sigma_x, \sigma_y, \sigma_z$ are the coordinate stresses, ν is Poisson's Ratio.

Under the conditions of steady state creep described above an analogous set of equations can be derived where the exponent of stress in the creep law is unity:

$$\frac{\partial \varepsilon_z}{\partial \phi} = \frac{\partial(\gamma + \alpha T)}{\partial \phi} + K[\sigma_z - \nu(\sigma_x + \sigma_y)] \qquad \text{eq. (5)}$$

where ϕ is irradiation dose γ is Wigner shrinkage deflection, K is creep coefficient per 10^{20} nvt. However the equation as it stands is not dependent upon irradiation dose level, although this is important if it varies across the plane of the brick. If the time dependent version of equation (5) is considered:

$$\frac{\partial \varepsilon_z}{\partial t} = \frac{\partial(\gamma + \alpha T)}{\partial t} + K\frac{\partial \phi}{\partial t}[\sigma_z - \nu(\sigma_x + \sigma_y)] \qquad \text{eq. (6)}$$

Relating this to a mean dose level $\bar{\phi}$:-

$$\frac{\partial \varepsilon_z}{\partial t}\cdot\frac{\partial \phi}{\partial \bar{\phi}}\cdot\frac{\partial \bar{\phi}}{\partial t} = \frac{\partial(\gamma + \alpha T)}{\partial \phi}\cdot\frac{\partial \phi}{\partial \bar{\phi}}\cdot\frac{\partial \bar{\phi}}{\partial t} + K\frac{\partial \phi}{\partial \bar{\phi}}\cdot\frac{\partial \bar{\phi}}{\partial t}[\sigma_z - \nu(\sigma_x + \sigma_y)] \qquad \text{eq. (7)}$$

which gives

$$\frac{\partial \varepsilon_z}{\partial \bar{\phi}} = \frac{\partial(\gamma + \alpha T)}{\partial \phi}\cdot\frac{\phi}{\bar{\phi}} + K\frac{\phi}{\bar{\phi}}[\sigma_z - \nu(\sigma_x + \sigma_y)] \qquad \text{eq. (8)}$$

The mean dose $\bar{\phi}$ is an arbitrary level and can be considered as unity, therefore:

$$\frac{\partial \varepsilon_z}{\partial \phi} = \frac{\partial(\gamma + \alpha T)}{\partial \phi}\cdot\phi + K\phi[\sigma_z - \nu(\sigma_x + \sigma_y)] \qquad \text{eq. (9)}$$

This equation is analogous to equation (4) where

$$\alpha T \equiv \frac{\partial(\gamma + \alpha T)}{\partial \phi}\cdot\phi$$

and $$\frac{1}{E} \equiv K\phi$$

The finite element program can therefore be used to find the stress levels appropriate to equation (9) using a distribution of artificial temperatures as input to the programe, such that when these temperatures are multiplied by the arbitrary value of coefficient of thermal expansion, magnitudes appropriate to $\frac{\partial(\gamma+\alpha\tau)}{\partial\phi}.\phi$ are obtained. To perform this analysis the lengthy procedure of defining the material property KØ for each element of the mesh is necessary.

Figure 6 shows the stress distribution appropriate to a late life peripheral fuel column at a level of 60% from the top of the active core using the above analysis for conditions of plane strain. It is seen that the resulting stress distribution is very similar to that obtained for a normal thermal elastic stress case. This is a result of the temperature dependence of the variation of shrinkage with irradiation dose.

5. BOWING OF BRICK COLUMNS

The peripheral fuel columns of the core undergo significant across brick fast neutron flux variations in the radial direction. This applies particularly to those fuelled columns with reflector columns on three adjacent sides. This results in bowing of the individual bricks of these columns and hence, as all the bow is in the same direction, an overall accumulated column bow. For all rings of columns inboard from this peripheral ring the extent of column bowing is small in comparison with the inter-column gap. In addition significant damage dose gradients exist across some of the inner side reflector columns (i.e. those columns immediately surrounding the peripheral fuelled columns) since the dose falls off substantially to zero on the outer side of these columns.

As the B.N.D.C. core is designed to have non-interacting fuel columns, the amount of column bow is clearly an important design parameter.

The method of calculation is to assume that each block of a column distorts an amount which is determined only by the free extreme fibre length changes which result from differential Wigner shrinkage, thermal expansions and creep rates. The brick is auumed to be constrained in shape so as to bow uniformly over its length. The brick bow is then simply obtained and the additive effect of individual brick bow on the total column bow can be obtained assuming the column to be pin jointed at the core location planes beyond the top and bottom ends of the fuelled length.

The bow of an individual brick is given by

$$H = \frac{L.D}{\delta L}\left(1 - \cos\left(\delta L/2D\right)\right) \qquad \text{eq. (10)}$$

where H is brick bow, L is brick length, D is distance across flats of brick, δL is extreme fibre differential length change.

As $\frac{\delta L}{2D}$ is small and since: $\cos(x) = 1 - \frac{x^2}{2!} + \frac{x^4}{4!} \ldots\ldots$ eq. (11)

$$H \approx \frac{L.\delta L}{8D}. \qquad \text{eq.(12)}$$

Calculation results are shown in Table 1 for the 'worst' peripheral fuel column (i.e. that column experiencing the greatest fast flux gradient) with fast neutron flux levels on extreme faces of 2.9 and 1.2 x 10^{21} n.v.t. Equivalent Dido Nickel dose. B1 to B6 refer to brick end face positions numbering from the bottom of the active core. Two further effects can affect the magnitude of column bow. These are out-of-squareness of the end faces of the individual bricks and brick "stepping" which results from non-central location between brick spigot and mating hole at brick interfaces. These effects are added to the peak column bow figures to give the maximum column bow. The intercolumn gap is then selected allowing some margin over the maximum column bow calculated as described above, in order to ensure that the core will remain non-interacting throughout the normal operating life of the fuel bricks.

For the 'worst' inner side reflector column, i.e. one adjacent to fuel columns on three sides and reflector columns on three sides the column bows at junctions B1 to B6 are shown in Table II for brick dwell times in the reactor of two, three and five years. It is seen in this case that longer dwell times can be allowed for the reflector columns compared with the average fuel column dwell time of two years, before interaction takes place between columns.

6. BRICK AND END FACE DISTORTION

Peripheral fuel columns are subjected to both temperature and irradiation dose gradients in radial directions. These will result in differential axial shrinkage across the end faces of the column bricks with the attendant possibility of edge gaps forming which may provide coolant leakage paths between abutting end faces.

The end face of the brick is divided into 45 representative areas to which are assigned irradiation dose levels and temperatures. Unrestrained Wigner shrinkages are then obtained for each of these areas. In addition thermal expansion strains are calculated and the differences between these parameters give an effective free shrinkage strain ϕ which varies over the end of the brick.

Now if ε_o is an overall shrinkage strain of the brick end face and $\pm\varepsilon'$ an average linear gradient of shrinkage varying from ε' to $-\varepsilon'$ at the brick edges then it can be seen that:

$$\phi_x = \varepsilon_o + \varepsilon'\frac{x}{a} + \varepsilon''_x \qquad \text{eq. (13)}$$

where a is half the distance across the brick, x is a coordinate distance along the face of the brick with x = o at the centre and ε'' is an elastic strain at the coordinate position x.

Now at the surface there is no resultant elastic strain and no resultant moment and so:

$$\int \varepsilon''_x \, dA = 0 \qquad \text{eq.(14)}$$

and

$$\int \varepsilon''_x E x \, dA = 0 \qquad \text{eq.(15)}$$

where dA is an elemental area of the surface and E is Young's Modulus.

Therefore integrating (13) with respect to area:

$$\int \phi_x \, dA = \int \varepsilon_0 \, dA + \int \varepsilon' \frac{x}{a} \, dA + \int \varepsilon''_x \, dA. \qquad \text{eq.(16)}$$

and so from equations (14),(15) and (16):

$$\varepsilon_0 = \int \phi \, dA / A \quad \text{since} \quad \int x \, dA = 0$$

Similarly:

$$\int \phi_x x \, dA = \int \varepsilon_0 x \, dA + \int \varepsilon' \frac{x^2}{a} \, dA + \int \varepsilon''_x x \, dA. \qquad \text{eq.(17)}$$

and so $$\varepsilon' = a \int \phi_x x \, dA \Big/ \int x^2 \, dA. \qquad \text{eq.(18)}$$

Therefore ε_0 and ε' can be calculated and hence from equation (13) the resultant surface strains ε''_x for each elemental area of the brick end face.

These surface strains are assumed to decrease linearly with depth into the brick until at some point they are entirely replaced by internal stresses. This distance is pessimistically assumed to be half the length of the brick.

Two positions in the worst peripheral fuel column have been analysed at levels 60% and 80% from the top of the active core. The results are shown in Figures 7 and 8 where the numbers given are actual gaps between two abutting end faces and not just distortions of one face. The values of gaps have been slightly adjusted to allow for creep under the stack load. The area of contact assumed for calculation of creep is pessimistically taken to be half the area of the end face. The effect of end face flatness tolerance is not included in the figures quoted.

7. CONCLUSIONS

The analyses discussed above enable the thermal and irradiation behaviour of the fuel bricks and columns to be determined. These analyses indicate also the mechanical and irradiation properties required of the graphite to be used for fuel bricks. clearly a material which exhibits low shrinkage under irradiation is desirable to limit column bowing and brick and face distortion to a minimum. It can also be seen from the foregoing discussion that the principal stresses occurring in the fuel bricks during normal operation of the reactor, derive mainly from differential thermal strains supplemented by other internal strains produced by irradiation induced shrinkage.

References

1. Lowthian C.S., Tyrrell J.F., "Advances in Current Gas Cooled Reactor Design in the U.K.", International Nuclear Industries Fair, Basel, Switzerland. 6 - 11 October 1969.

2. Insch G.M., Thorn J.D., Hurst J.N., "The H.T.R. - Choice of Style and Performance", International Nuclear Industries Fair, Basel, Switzerland. 6 - 11 October 1969. Technical Meeting No. 3/9.

3. Miles G.A., White D.J., "The Finite Element Method and its Applications in an Engineering Laboratory", Journal of Science and Technology, Vol.37, No.3, 1970.

TABLE I

Bow of a Peripheral Fuel Column After 2 Years

Bow at block junctions in mm.					
B1	B2	B3	B4	B5	B6
1.57	8.5	12.4	11.6	7.1	0.88

TABLE II

Bow of an Inner Side Reflector Column

Dwell Time	Bow at block junctions in mm.					
	B1	B2	B3	B4	B5	B6
2 yrs	1.1	5.1	6.2	4.7	2.4	0.1
3 yrs	2.0	10.2	12.3	10.4	5.5	0.4
5 yrs	3.7	19.8	27.3	23.9	14.0	1.5

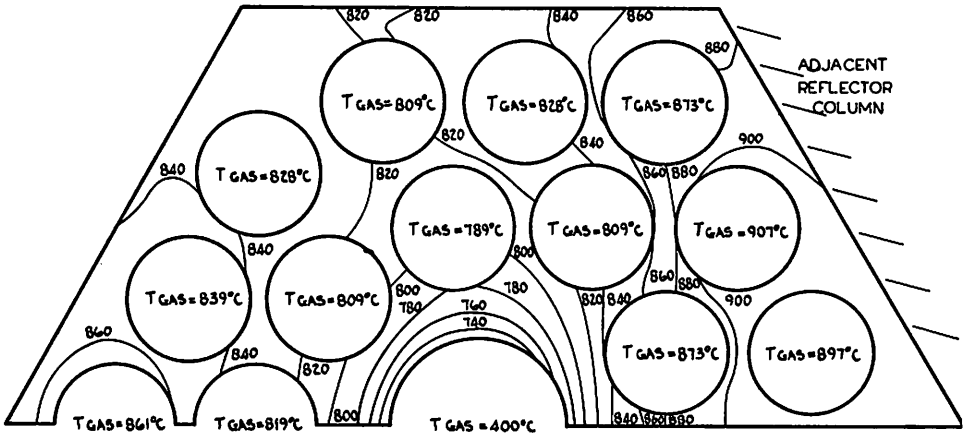

Fig.1 Temperature distribution for early life peripheral fuel column at the bottom plane of the active core for the case of partial withdrawal of the control rod.

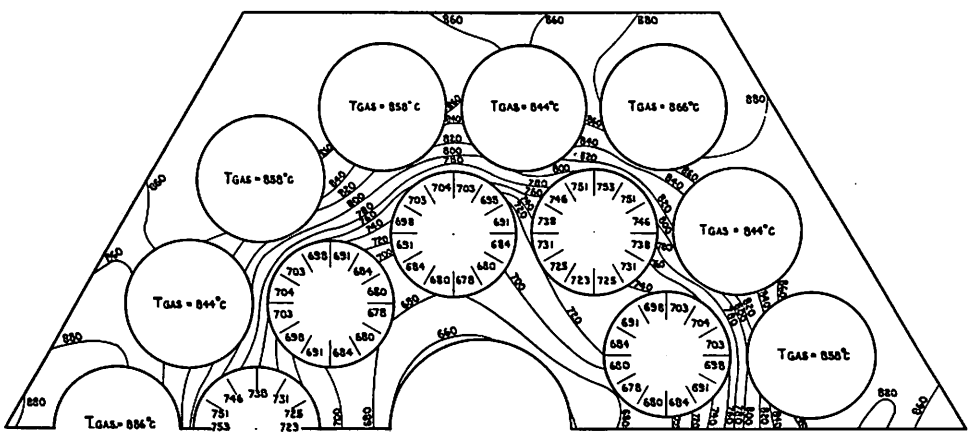

Fig.2 Temperature distribution for early life centre column at the bottom plane of the active core with full control rod insertion.

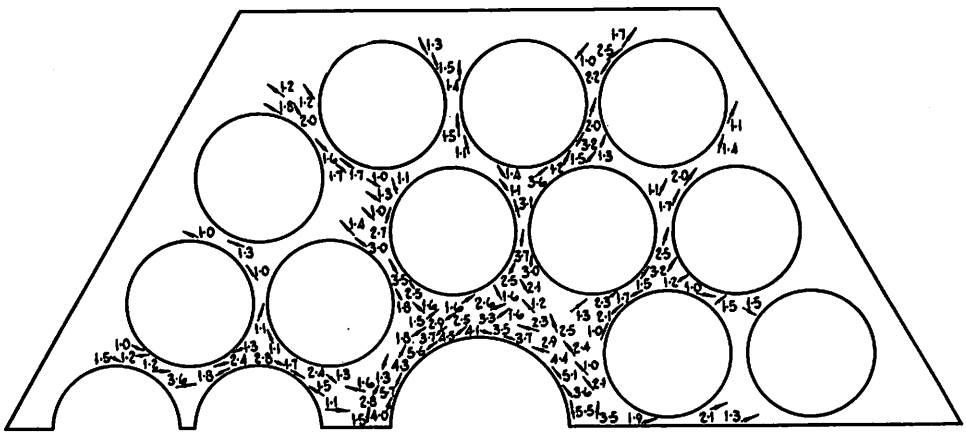

Fig.3 Thermal stress distribution based on temperatures of Fig.1 for conditions of plane strain. Principal tensile stresses plotted in N/mm^2.

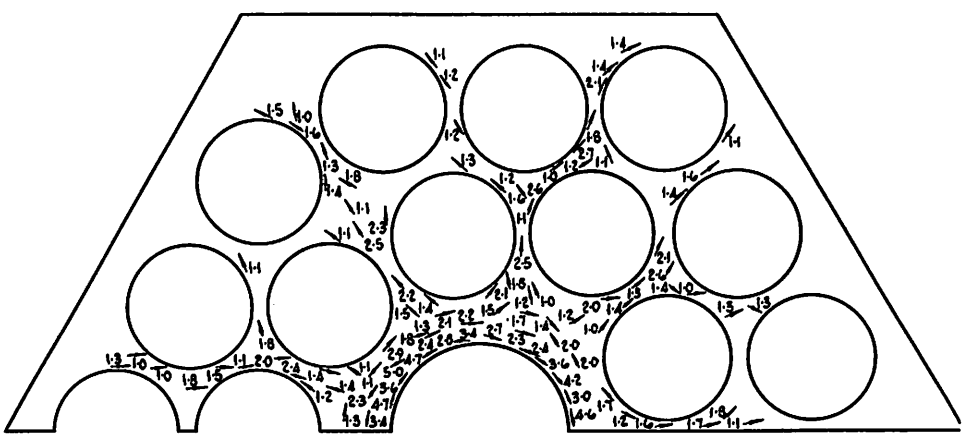

Fig.4 Thermal stress distribution based on temperatures of Fig.1 for conditions of plane stress. Principal tensile stresses plotted in N/mm^2.

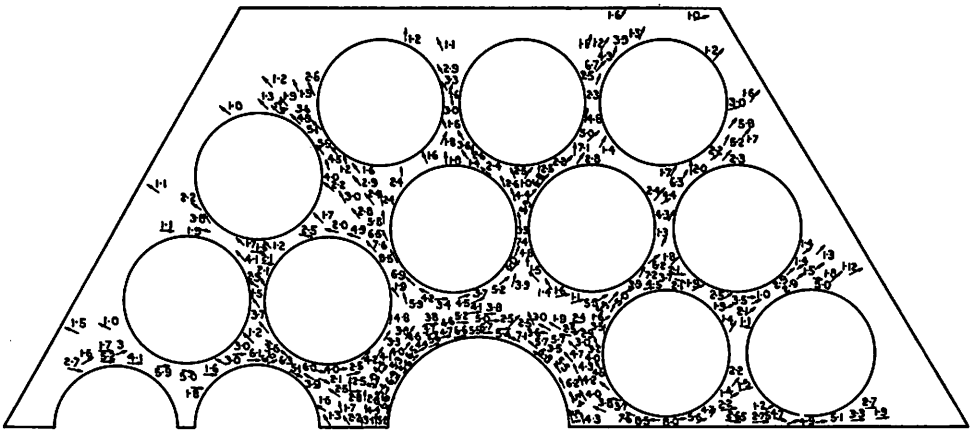

Fig.5 Thermal stress distribution based on temperatures of Fig.2 for conditions of plane strain. Principal tensile stresses plotted in N/mm^2.

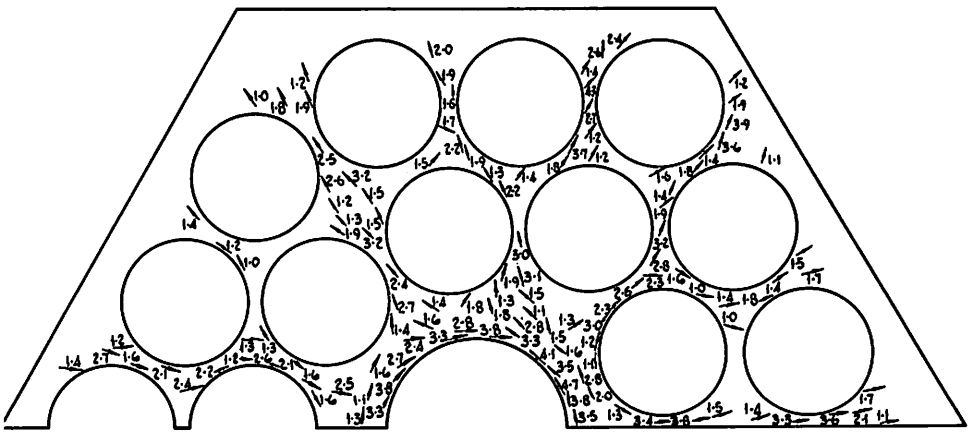

Fig.6 Stress distribution for peripheral fuel column at a plane 60% from the top of the active core resulting from differential irradiation induced shrinkage and creep for conditions of plane strain. Principal tensile stresses plotted in N/mm^2.

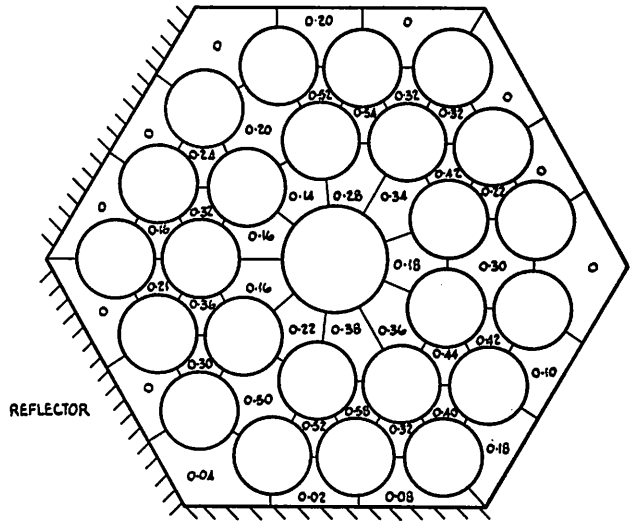

Fig.7 Distribution of distortion produced gaps at a brick interface 60% distance from the top of the active core.

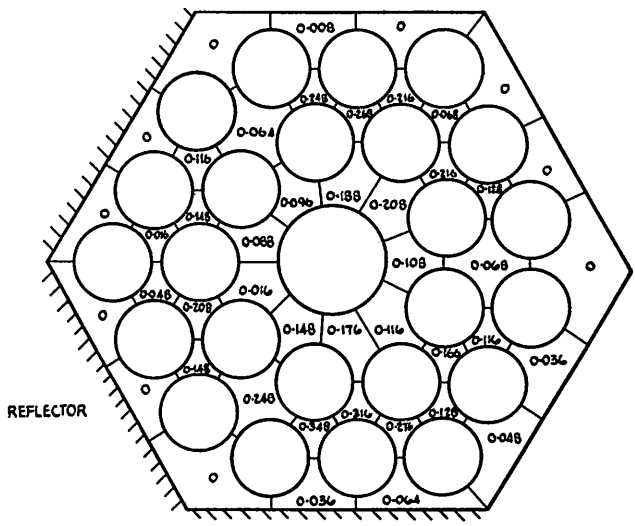

Fig.8 Distribution of distortion produced gaps at a brick interface 80% distance from the top of the active core.

DISCUSSION

Q A. N. KINKEAD, U. K.

Although I have not seen Mr. Beckett's paper, I noticed that the maximum stress occurring around the control rod channel for a rod withdrawn case at 60% core depth appeared to have a value of around 5.5 N/mm^2 tensile both at start of life and end of life. Was the end of life state that at shutdown of the reactor or did I miss some of Mr. Beckett's comments on this problem ?

A V. BECKETT, U. K.

The stresses shown for the 60% core depth was for late fuel life conditions and resulted from differential irradiation induced shrinkages at operating conditions and showed tensile hoop stresses around the central hole.
This should not be confused with the distribution for early life conditions. Here the stresses result from a different cause, that of temperature gradients producing thermal elastic stresses. These stresses are assumed to disappear after a short irradiation dose due to enhanced creep rates.